

Efficient synthesis of new tetrazole-based sulfonamide derivatives: cytotoxicity and molecular docking studies on HT29 cancer cell line

Zahra Sadeghi^a, Zohreh Mirjafary^{*a}, Hoda Abolhasani^{b,c}, Gholamreza Najafi^d, Fatameh Heidari^{b,e}

^aDepartment of Chemistry, Science and Research Branch, Islamic Azad University, Tehran, Iran
zmirjafary@srbiau.ac.ir

^bCellular and molecular research center, Qom University of Medical Sciences, Qom, Iran

^cDepartment of physiology & Pharmacology, Faculty of Medicine, Qom University of Medical Sciences, Qom, Iran

^dDepartment of Chemistry, Qom Branch, Islamic Azad University, Qom, Iran

^eDepartment of Anatomy, Faculty of Medicine, Qom University of Medical Sciences, Qom, Iran

Received: September 2023; Revised: September 2023; Accepted: October 2023

Abstract: In this study, two novel tetrazole-based sulfonamide derivatives, N-((2H-tetrazol-5-yl)methyl)(phenyl)-N-tosylmethanamine (**5a**) and N-((2H-tetrazol-5-yl)methyl)-N-tosylpyridin-2-amine (**5b**) were synthesized through an azide-nitrile cycloaddition reaction. The reaction proceeded smoothly in good yields (70-78%) using ZnBr₂ as a robust catalyst and H₂O/2-propanol as a green solvent system. The structure of the products was confirmed by FT-IR, ¹HNMR, ¹³CNMR, and LC-Mass analysis. Cytotoxicity evaluations of **5a** and **5b** on HT29 cell line demonstrated that compound **5b** has the most potent *in vitro* antiproliferative activity with IC₅₀ values of 24.66 ± 4.51 μM. Although, compound **5a** showed anti-proliferative activity with IC₅₀ values of 85.57 ± 6.61 μM on HT29 cells, comparable to Cisplatin, as a potent known anticancer drug with IC₅₀ values of 7.49 ± 1.71 μM. Furthermore, we performed molecular docking studies to investigate the possible drug-likeness of the synthesized molecules **5a** and **5b**, from which the results suggested that compound **5b** could be a promising candidate for p53 inhibition.

Keywords: Tetrazole, Sulfonamides, [2+3] Cycloaddition, Cytotoxicity, colorectal cancer, HT29 cancer cell line, Molecular docking studies.

Introduction

Colorectal cancer is a significant global health concern, ranking as the second most deadly malignancy worldwide. However, this disease is accompanied by various drawbacks and limitations, including increased toxicity, resistance, and a lack of selectivity towards cancer cells. Consequently, there is a need to explore innovative approaches and novel chemotherapeutic agents to address these challenges [1].

Many researches have been conducted on the material's antioxidant, cytotoxicity, and anti-colon cancer properties through various

biological assays. Colorectal cancer (CRC) is a pervasive and aggressive form of cancer that impacts the gastrointestinal system, making it the second most common cause of cancer-related fatalities worldwide [2, 3]. Nevertheless, the existing treatments for CRC often result in severe side effects such as incision area swelling or bruising, nerve damage, toxicity, hair loss, fatigue, and diarrhea. Consequently, researchers have been actively seeking new formulations to overcome these issues. Recently, metal nanoparticles have gained attention as unconventional formulations due to their excellent anticancer properties without causing adverse effects [4]. Cancer stands as a grave peril to global human well-being. The development of

*Corresponding author: Email: zmirjafary@srbiau.ac.ir

cancer is a complex process, characterized by the uncontrolled growth of abnormal cells that invade surrounding tissues, serving as a fundamental pathway in cancer progression. Numerous strategies have been proposed to inhibit nuclear and cellular division, ultimately affecting the mitotic spindle and emphasizing microtubules as essential molecular targets for the advancement of anticancer therapies [5-9].

In recent years, numerous mechanisms have been proposed for the effectiveness of anti-cancer drugs. One such mechanism involves tetrazole-based drug candidates, which have shown promising anti-cancer potency through various pathways. These pathways include the inhibition of COX-2 and PRMT, as well as the regulation of tubulin polymerization, angiogenesis, efflux pump, and HIF-1 α . Additionally, tetrazole-based analogs have been found to modulate the expression of Bcl-2, Ki-67, and caspases, leading to cell cycle arrest and apoptosis. In a study conducted by Zhang *et al.* in 2019, the structure-activity relationship (SAR) of tetrazole substituted hybrids was briefly discussed [10]. Furthermore, our recent research involved the *in silico* investigation of tetrazoles using docking studies, specifically focusing on a compound called N-((2H-tetrazol-5-yl) methyl)-4-methyl-N-tosylbenzamine [11]. The findings of this study were consistent with the anticancer effect observed in a selective COX-2 inhibitor called celecoxib [11-16]. Moreover, the catalytic synthesis of 1-substituted-1H-tetrazoles and *in vitro* studies on their cytotoxicity and anti-colorectal adenocarcinoma effects on HT-29 cell lines have been conducted [17]. The physicochemical and pharmacological properties of tetrazole compounds such as Ceftezole and Zotarolimus have been investigated, both of which have demonstrated high effectiveness against *in vivo* antitumor Xen-grafts [18]. Microcrystalline tetrazole cellulose (MCTC) (4) demonstrated remarkable *in vitro* antitumor activity against hepatic and breast tumor cells, including HCT-116, HeG2, and MDA-MB-231 (Fig1) [19].

The synthesis and SAR (structure-activity relationship) studies of novel 1, 2, 4-oxadiazole-sulfonamide-based compounds as potential agents for colorectal cancer therapy have been investigated [20]. Furthermore, the researchers explored the potential of novel sulfonamide analogs of 6/7-aminoflavones as anticancer agents through topoisomerase II inhibition [21]. Lastly, the evaluation encompassed new

sulfonamide-containing aminophosphonate and pyrazolo phosphate derivatives as selective COX-2 inhibitors and promising candidates for anti-tumor therapy [22, 23].

Another study conducted by Mokenapelli *et al.* evaluated the anti-proliferative activity of novel benzofuran based tetrazole hybrids (5) against two human cancer cell lines, HCT116 and Miapaca2, which represent colon and pancreatic cancer, respectively. The results of this study were illustrated in Fig. 1 [24]. Additionally, Romagnoli *et al.* assessed the growth inhibition of six different human cancer cell lines (HeLa, A549, HL-60, Jurkat, MCF-7, and HT-29) using 1,5-diaryltetrazoles (6) [25]. These findings contribute to the understanding of novel compounds and their potential applications in cancer treatment.

Tetrazoles are a type of aromatic heterocycles with an unsaturated five-membered ring structure, consisting of one carbon and four nitrogen atoms [26]. The field of tetrazole chemistry has seen significant advancements in the search for new drugs and biologically active compounds [27]. One of the key advantages of tetrazole-containing compounds is their resistance to enzymatic degradation, as tetrazole does not naturally occur in biological sources [28]. The 1,3-dipolar cycloaddition of azide and nitriles is the most commonly used method for synthesizing tetrazoles [29, 30]. In medicinal chemistry, numerous bioactive compounds with tetrazole-based heterocyclic scaffolds have been developed [31, 32], exhibiting diverse efficacy such as anti-hypertensive [33, 34], anti-histaminic [35], anticancer [36, 37], anti-fungal [38], anti-inflammatory [39, 40], anti-asthmatic [41], and antimicrobial activity [42-44].

The tetrazole moiety has proven to be a valuable component in the development of different antineoplastic agents [10]. Additionally, drugs like Irbesartan [45], valsartan [46, 47], cefazolin [48, 49], and tomelukast [41, 50], that are based on tetrazole, have already been utilized in clinical settings (Fig. 2). Tetrazoles continue to attract significant attention from both academia and industry [51]. This heterocycle plays a crucial role in various fields such as energetic materials [52], supramolecular and coordination chemistry [53], organo catalysis [54], and medicinal chemistry [31, 55]. The interest in tetrazoles stems from their distinctive structure and properties [56]. In the realm of medicinal chemistry, the 5-substituted 1H-tetrazole unit is

frequently employed as a metabolism-resistant isosteric replacement for carboxylic acids [57, 58], Cl-amidine [59], cis amide [60], and furan ring [10] in structure-activity relationship (SAR) studies. Tetrazole, acting as a bioisostere of carboxylic acid, can engage in various non-covalent interactions such as hydrogen bonding and dipole interaction, thereby enhancing the physicochemical properties and the ability to bind to biomolecular targets [61, 62].

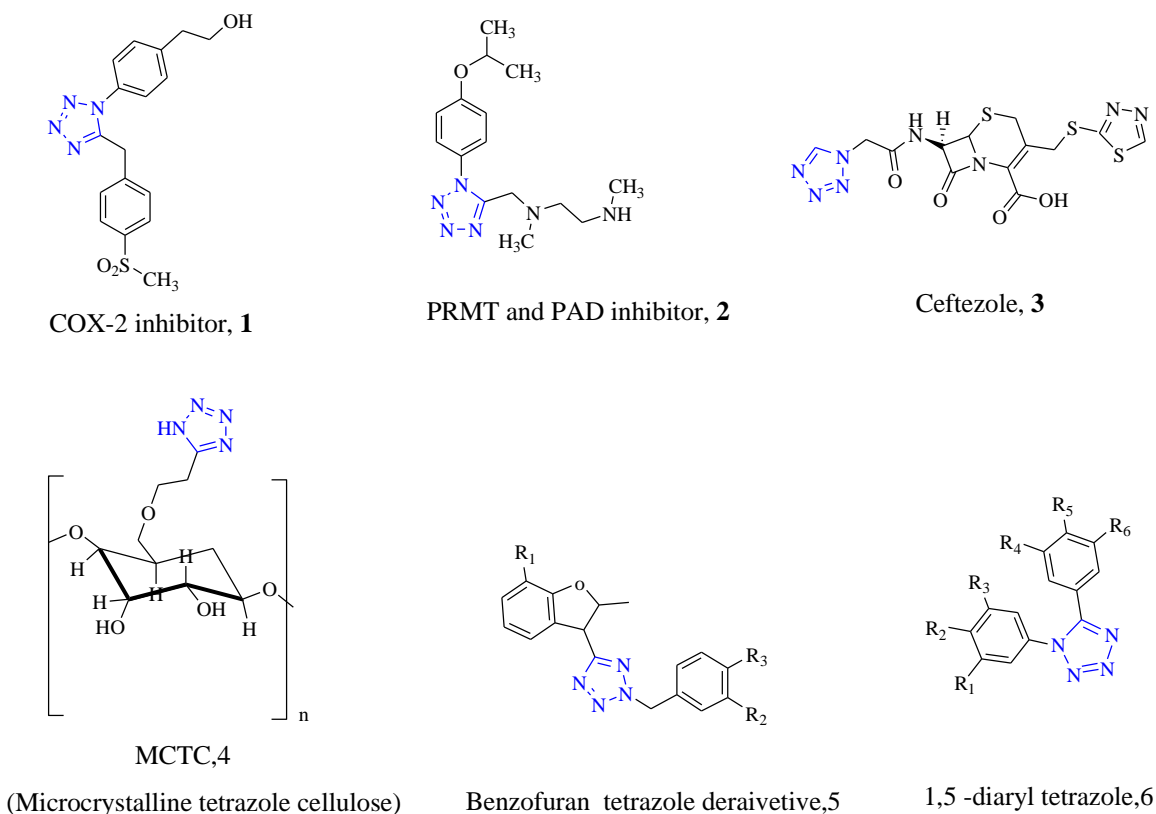


Fig. 1. Chemical structure of COX-2 inhibitors **1** and PRMT and PAD inhibitor **2**; anticolon cancer agents Ceftazole **3**, MCTC (Microcrystalline tetrazole cellulose) **4**, anti-proliferative activity cell lines HCT116 and Miapaca2 benzofuran based tetrazole derivative **5**, 1,5-diaryltetrazoles **6**.

Generally, the presence of the tetrazole moiety induces an increased bio-availability activity without any toxicity enhancement [36, 63] of the active pharmaceutical ingredient [59, 64]. So, tetrazole derivatives play a pivotal role in

developing of new drugs [59] and numerous compounds containing a tetrazole moiety are currently on the pharmaceutical market (Fig. 2).

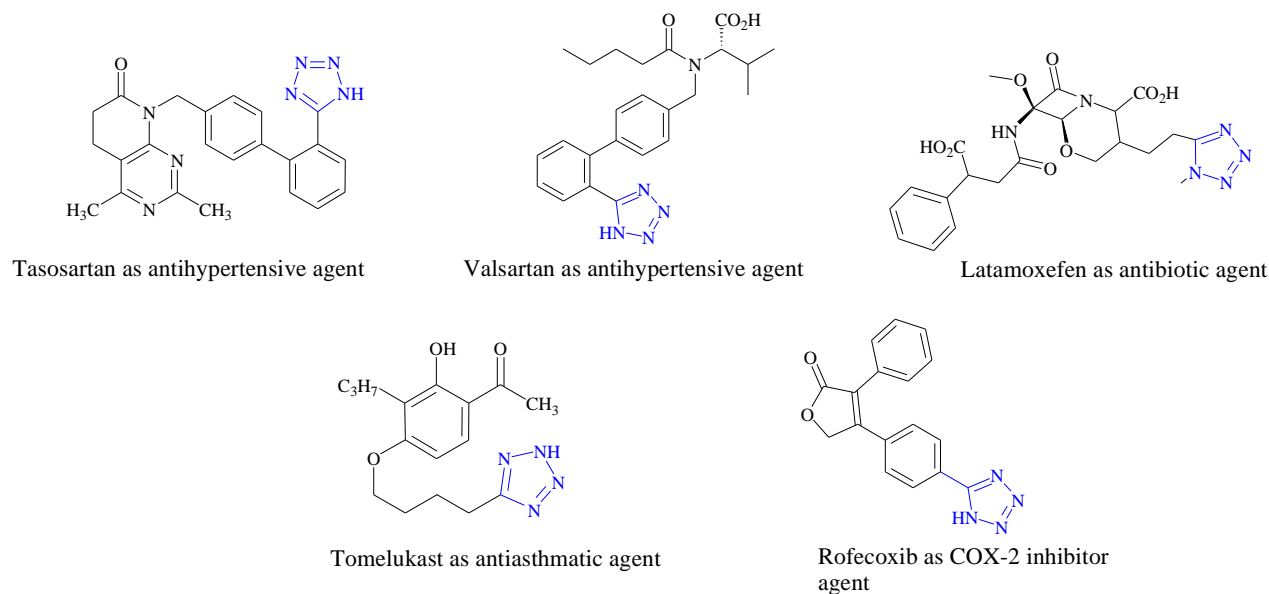


Fig. 2. Chemical structure of some known tetrazole-based drugs.

The initial part of this investigation involved the synthesis of novel tetrazole derivatives containing the biologically active sulfonamide group through a 1,3 dipolar cycloaddition reaction. Tetrazoles have demonstrated encouraging outcomes in the field of medicinal chemistry. Subsequently, the synthesized compounds were examined in the second section of the study to evaluate their potential anti-cancer activity. It is worth noting that targeted therapy, chemotherapy, and surgery remain the prevailing treatment approaches for individuals diagnosed with colorectal cancer [1].

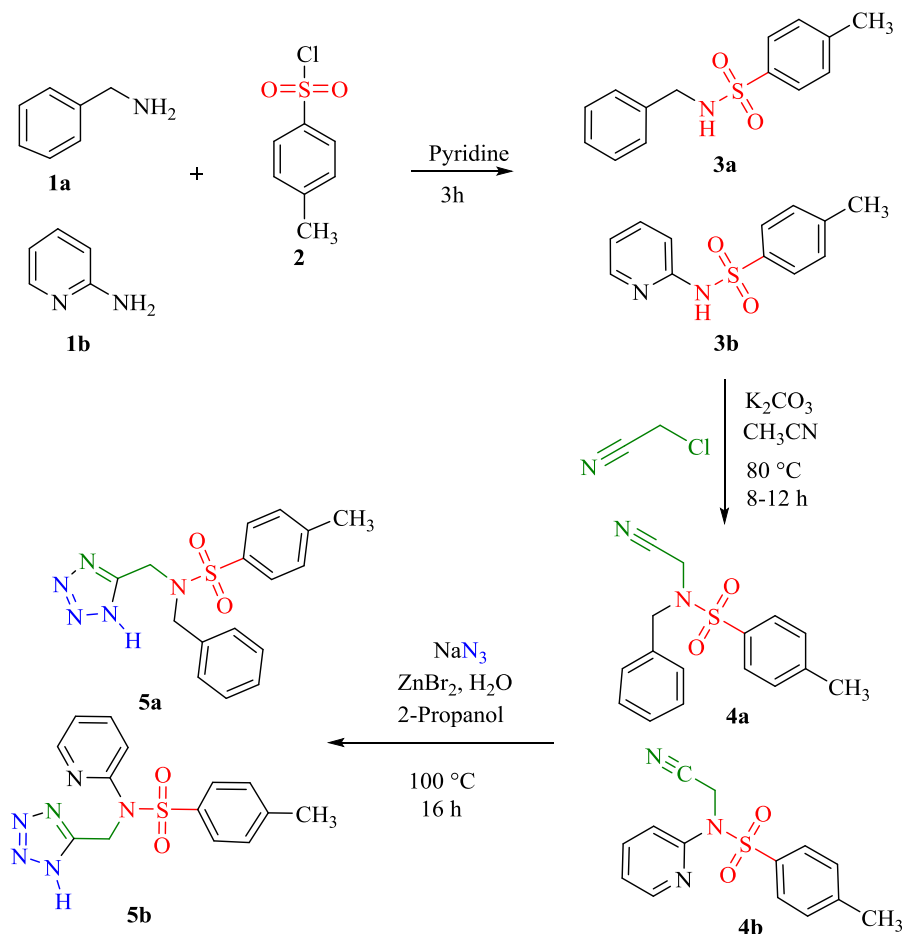
Results and Discussion

Chemistry

The synthesis of tetrazole compounds **5a-b** was carried out from the reaction of nitrile compounds **4a-b** with sodium azide, in the presence of zinc bromide ($ZnBr_2$) in the mixture of 2-propanol/ H_2O as solvent system. The products were confirmed by FT-IR, 1H NMR, ^{13}C NMR and LC-Mass analysis. Compounds **4a-b** were obtained according to previously reported method [11], by the reaction of substituted-*N*-tosylbenzenamines **3a-b** with chloroacetonitrile in the presence of K_2CO_3 in acetonitrile as solvent. Substituted-*N*-tosylbenzenamines **3a-b** were prepared by the reaction of 4-

methylbenzene-1-sulfonyl chloride **2** in pyridine with amines **1a-b** (Scheme 1).

The new synthesized 5-substituted tetrazole compounds **5a** and **5b** were characterized by FT-IR, 1H NMR, and ^{13}C NMR analysis. The observed peak for the N-H bands (3400 cm^{-1}) in sulfonamide **3a** will be disappeared in the corresponding nitrile compound **4a** after the reaction with chloroacetonitrile, which led to a new signal at 2200 cm^{-1} related to the CN band. The absence of the CN peak and the presence of new N-H absorptions (3400 cm^{-1}) related to tetrazole in the IR spectra of **5a** confirmed the azide-nitrile reaction. In 1H NMR spectra, the chemical shift (δ) observed for the singlet peak of NH proton in sulfonamide **3a** changes from 10.2 ppm to 15.7 ppm (NH tetrazole) in product **5a**, proving the favored cyclization. Moreover, the singlet peak of CH_2 protons in nitrile compound **4a** at δ 4.86 ppm was converted to a singlet peak at δ 5.12 ppm in compound **5a**, confirming the [2+3] cyclization. ^{13}C NMR experiment of **5a** allowed complete assignment of two aliphatic carbons at $\delta = 21.44$ and 43.46 ppm and eleven aromatic carbon signals at $\delta = 120.70$ - 153.36 ppm.



Scheme 1. Efficient synthesis of tetrazole derivatives **5a-b**.

Molecular docking studies

The synthesized molecules **5a** and **5b** were subjected to analysis on proteins 2W96 and 5LAP, utilizing our molecular docking results. Through this analysis, we determined that the binding affinities of **5b** were -8.23 kcal/mol and -6.28 kcal/mol for 5LAP and 2W96, respectively. The 5LAP protein, known for its high mutation rate in human cancers, acts as a tumor suppressor for p53. Mutated forms of p53 that promote tumor growth are often unstable and accumulate quickly, making them vulnerable to stabilization through pharmacological intervention [68]. Based

on our molecular docking findings, compound **5b** exhibits potential as a promising candidate for inhibiting p53, as indicated in Table 1.

In addition, the 2W96 protein controls the CDK4-cyclin D1 complex, which plays a vital role in regulating the G (1) phase of cell cycle progression. It is worth noting that the dysregulation of CDK4/cyclin D1 signaling greatly contributes to the development of cancer [69]. The results obtained from molecular docking experiments indicate that **5b** exhibits the ability to inhibit both p53 and CDK4/cyclin D1, thereby positioning it as a potential and hopeful candidate for the treatment of colorectal cancer.

Table 1. Protein names, the related PDB ID, and their control molecules for molecular docking studies.

Protein Name	PDB ID	Control molecule
p53-compromised cells	5LAP	2-Sulfonylpyrimidines
CDK4	2W96	Cyclin D

Table 2. Molecular docking interactions of the synthesis and control molecules (kcal/mol).

Compound ID	Protein PDB ID	
	5LAP	2W96
5a	-6.13	-5.27
5b	-8.23	-6.28
2-Sulfonylpyrimidines	-15.83	
Cyclin D	-18.58	

In vitro growth inhibition assay

Previous studies have demonstrated that certain tetrazole derivatives containing sulfonamide exhibit antiproliferative activity, potentially through a mechanism similar to that of colchicine [70, 71]. The efficacy of tetrazole derivatives in the treatment of colorectal and breast cancer has been extensively investigated [36]. In this particular study, the MTT assay was employed to assess the inhibitory effect of the designed compounds (5a and 5b) on the growth of human colorectal adenocarcinoma cell lines (HT-29). The IC₅₀ values, obtained by fitting the

data into sigmoidal concentration-response curves using non-linear regression analysis for each cell line (Fig.3), were presented in Table 3. The results revealed that the cytotoxicity of the investigated compounds varied significantly depending on the cell type used in the MTT assay. Notably, the compounds exhibited lower toxicity towards HT-29 cells, suggesting that they may possess more promising anti-colorectal cancer effects. However, further in vitro and in vivo studies are necessary to validate this conclusion.

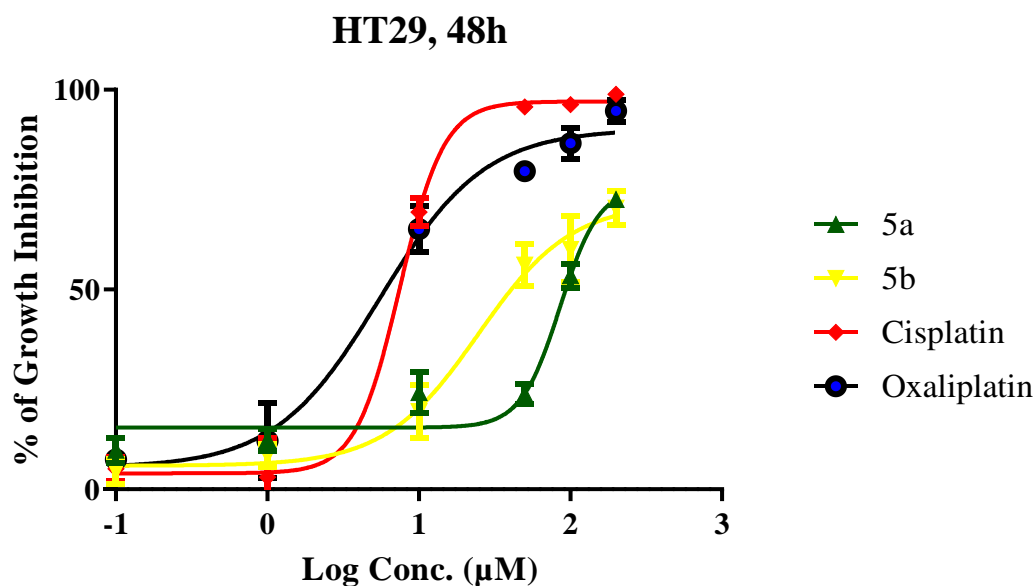


Fig. 3. Plot of the percentage of growth inhibition at different concentrations of compounds **5a** and **5b**, and anticancer drugs (Cisplatin, Oxaliplatin) on HT29 cell line, determined by MTT assay after an incubation time of 48 h. Data were fitted into sigmoidal dose-response curves using non-linear regression analysis. Values represent mean \pm RSD of at least three determinations.

The cytotoxicity evaluations of compounds **5a** and **5b** on HT29 cancerous cell lines demonstrated interesting findings. Compound **5b** exhibited the most potent in vitro antiproliferative activity, as it displayed IC₅₀ values of $24.66 \pm 4.51 \mu\text{M}$ on HT29 cells. This indicates its potential as a promising candidate for further investigation. On the other hand, compound **5a** also exhibited anti-proliferative activity with IC₅₀ values of $85.57 \pm 6.61 \mu\text{M}$ on HT29 cells, which is comparable to the well-known anticancer drug Cisplatin. The MTT assay was employed to evaluate the antiproliferative activity of both compounds, as well as other effective anticancer drugs such as Oxaliplatin and Cisplatin, against the HT29 cell line. To determine the IC₅₀ values, non-linear regression analysis was utilized by fitting the data into a sigmoidal dose-response curve (Fig. 3). The cytotoxicity evaluation results for compounds **5a** and **5b**, along with the anticancer drugs, are presented in Table 3. These findings contribute to the understanding of the potential antiproliferative activity of these compounds and their comparison to established anticancer drugs.

Table 3. Anti-proliferative activities (IC₅₀) of the compounds **5a**, **5b**, cisplatin, and oxaliplatin against HT29 cell line after 48 h treatment.

Compound	HT 29 ^a
	IC ₅₀ ± RSD (μM)
5a	85.57 ± 6.61
5b	24.66 ± 4.51
Cisplatin	7.49 ± 1.71
Oxaliplatin	5.52 ± 1.41

^aIC₅₀, concentration of drug required for 50% inhibition of cell growth measured by MTT assay. Cells were treated with compounds for two days (48h). IC₅₀ values are the mean ± RSD (relative SD = [SD/average]*100) of at least three determinations.

Conclusion

To summarize, the synthesis of novel tetrazole compounds **5a-b** was documented by reacting N-methylene nitrile sulfonamides **4a-b** with sodium azide in the presence of ZnBr₂. Subsequently, an examination of their biological properties was conducted. The findings indicated that N-((2H-tetrazol-5-yl) methyl)-N-tosylpyridin-2-amine **5b** serves as a promising framework for the development of novel anticancer agents with antiproliferative activity.

Experimental

Materials and Instrument

All reagents and solvents were purchased from the Aldrich or Merck Chemical Companies and used without further purifications. Culture media (RPMI 1640), Trypan blue, FBS (Fetal Bovine Serum), PBS (Phosphate Buffered Saline), Pen/strep (penicillin/streptomycin solution), and Trypsin-EDTA solution were provided by Sigma-Aldrich Company. MTT [3-(4, 5-dimethylthiazol-2-yl) 2,5-diphenyl tetrazolium bromide], dimethyl sulfoxide (DMSO), glycine, and NaCl were obtained from Sigma Aldrich Chemical Co. Cisplatin-Lösung Ribosepharm 10 mg (0.5 mg/mL), Oxaliplatin Nanoalvand (Alvoxal 50) (50 mg/10 mL) was purchased from the local market.

Melting points were determined using a Thomas Hoover capillary apparatus (Philadelphia, USA). The reactions were monitored by thin-layer chromatography (TLC) with UV light and iodine, as detecting agents. Infrared spectra were acquired on a Perkin-Elmer 1420 ratio recording spectrometer in the range of 400-4000 cm⁻¹ area. A Bruker FT-250 MHz instrument (Brucker Biosciences, USA) was used to acquire ¹HNMR and ¹³CNMR spectra in DMSO-d₆ as solvents. LC-MS analysis was performed on an Agilent 1200 LC system to determine the molecular weight of **5a** and **5b**.

General procedure for preparation of phenyl-N-tosylmethanamine (3a) and N-tosylpyridin-2-amine (3b):

The sulfonamide **3a** and **3b** were prepared according to previously reported method (scheme 1) [11]. To a stirred solution of amine **1a-b** (5 mmol) in 3 mL pyridine, 4-methylbenzene-1-sulfonyl chloride (6 mmol) was added and stirred for 3 h at room temperature. After completion of the reaction, the mixture was poured into ice-cold water and stirred for 15 min, which resulted in the precipitation of the desired sulfonamide in a high yield (94-98%). The structures were confirmed by FT-IR, ¹HNMR and melting points.

phenyl-N-tosylmethanamine (3a): white crystalline powder (94%); mp: 109-110 °C; IR (KBr): 1162, 1324 (SO₂), 3268 (NH sulfonamide) cm⁻¹; ¹HNMR (250 MHz, DMSO): δ = 2.28 (s, CH₃), 7.02 (d, *J* = 7.7 Hz, 2H), 7.14 (d, *J* = 7.5 Hz, 2H), 7.20-7.61 (m, 5H), 10.17 (s,

NH sulfonamide).

N-tosylpyridin-2-amine (**3b**): light pink crystalline powder (%98); mp: 110-114 °C; IR (KBr): 1079, 1361 (SO₂), 3431 (NH sulfonamide) cm⁻¹.

General procedure for preparation of 2-(*N*-phenyl-*N*-tosylamino) acetonitrile (4a) and 2-(*N*-(pyridin-2-yl)-*N*-tosylamino) acetonitrile (4b):

According to previously reported method (11), to a stirred solution of the sulfonamide 3a-b (3 mmol) and K₂CO₃ (3 mmol) in acetonitrile (5 mL), chloroacetonitrile (3.3 mmol) was added dropwise (scheme 1). The reaction mixture was heated at 80° C for 8 h. After completion of the reaction, as monitored by TLC, the solvent was evaporated under vacuum. Water was added, and the reaction mixture was extracted by DCM (3 × 5 mL). The combined organic extracts were dried with Na₂SO₄, filtered, and evaporated to obtain pure compounds 4a-b in good yields.

2-(*N*-phenyl-*N*-tosylamino)acetonitrile (4a): white powder (65%); mp: 196-198 °C; IR (KBr): 1165, 1356 (SO₂), 2249 (C≡N nitrile) cm⁻¹.

2-(*N*-(pyridin-2-yl)-*N*-tosylamino)acetonitrile (4b):

white powder (68%); mp: 145-147 °C; IR (KBr): 1165, 1361 (SO₂), 2254 (C≡N nitrile) cm⁻¹.

General procedure for preparation of *N*-((2*H*-tetrazol-5-yl)methyl)(phenyl)-*N*-tosylmethanamine (5a) and *N*-((2*H*-tetrazol-5-yl)methyl)-*N*-tosylpyridin-2-amine (5b):

The synthesized compounds 4a-b (1 mmol), sodium azide (2 mmol), and zinc bromide (0.5 mmol) were dissolved in a mixture of 2-propanol/H₂O (1:1, 10 mL) and was refluxed for 16 h. After completion of the reaction, 5 mL of 10% citric acid and 30 mL of ethyl acetate were added, and stirring was continued until no solid remained. The organic phase was separated, and the aqueous layer was extracted twice with ethyl acetate. The combined organic layer was washed with water and dried over anhydrous Na₂SO₄. The solvent was removed under vacuum, and the desired product was separated by chromatography (EtOAc-hexane (1:4)). The structure of the products were confirmed by FT-

IR, ¹HNMR, ¹³C NMR, LC-Mass and melting points.

***N*-((2*H*-tetrazol-5-yl)methyl)(phenyl)-*N*-tosylmethanamine (5a):**

white powder (78%); mp: 117-119 °C; IR (KBr): 1159, 1335 (SO₂), 3269 (NH tetrazole) cm⁻¹; ¹HNMR (250 MHz, DMSO): δ = 2.35 (s, CH₃), 3.92 (s, CH₂), 4.40 (s, CH₂), 7.24 (broad s, 2H), 7.32 (d, J = 7.7 Hz, 2H), 7.64 (d, J = 7.0 Hz, 2H), 8.01-8.05 (t, J = 0.5 Hz, 3H), 16-17 (broad s, NH tetrazole); ¹³C NMR (DMSO, 63 MHz): δ = 21.30 (CH₃), 46.33 (CH₂), 52.12 (CH₂), 126.90, 127.40, 127.90, 128.26, 128.52, 128.90, 130.10, 130.30, 153.54 (C=N) ppm. [M-H]⁺ = 342 m/z.

***N*-((2*H*-tetrazol-5-yl)methyl)-*N*-tosylpyridin-2-amine (5b):**

white powder (70%); mp: 133-137°C; IR (KBr): 1167, 1360 (SO₂), 3444 (NH tetrazole) cm⁻¹; ¹HNMR (250 MHz, DMSO): δ 2.33 (s, CH₃), 5.27 (s, CH₂), 7.32 (d, J = 7.2 Hz, 2H), 7.52 (d, J = 6.5 Hz, 2H), 7.76-7.82 (dd, J = 7.0 Hz, 3H), 8.20 (broad s, 1H), 16-17 (broad s, NH tetrazole); ¹³CNMR (DMSO, 63 MHz): δ 21.44 (CH₃), 43.46 (CH₂), 120.70, 122.30, 127.81, 130.35, 134.80, 138.90, 144.90, 148.48, 153.36 (C=N) ppm. [M+H]⁺ = 331 m/z.

Cell culture

HT29 cancerous cell line was provided by Pasteur Institute of Iran (Tehran) and was grown adherently in RPMI 1640 media, which was supplemented with 10% (v/v) fetal bovine serum, L-glutamine (2 mM), Penicillin G-Streptomycin (100 U/ml and 100 µg/ml), under a 5% CO₂ atmosphere at 37°C in a humidified incubator.

Different concentrations (i.e., 0.1 µM, 1 µM, 10 µM, 50 µM, 100 µM, and 200 µM) of compounds 5a and 5b, and Cisplatin and Oxaliplatin were prepared. The stock solutions of compounds 5a and 5b, (1 mg/100 µL) were prepared in DMSO. The stock solutions of Oxaliplatin (5 mg/1 mL) and Cisplatin (0.5 mg/1 mL) were used as the injection solutions. Subsequently, proper quantities of the stock solutions (depending on molecular weight) were mixed with 1 mL of the culture media to reach a concentration of 100 µM, from which the other dilutions of compounds and standard drugs were obtained. Positive control (1 mM H₂O₂) was obtained by adding 11 µL of 3% H₂O₂ stock solution to 10 mL of the culture media. Negative control was just the medium with no drug.

Afterward, each concentration was exposed to cell lines for a minimum of 48 h in three wells.

Anti-proliferative assay

The cytotoxicity activities of compounds 5a and 5b, Oxaliplatin, and Cisplatin against the HT29 cell line were determined using the MTT assay. Cell count and viability were assessed through trypan blue staining followed by hemocytometry. Only cultures at 90% confluency were utilized for the experiments. The cells were always utilized within two weeks after being removed from liquid nitrogen storage. For the experiments, all cells were seeded at a density of 5000 cells per well of 96-well plates in 200 μ L medium and allowed to attach for 24 hours (pre-incubation). Once a partial monolayer of cells was formed, the supernatant was removed, and 200 μ L of medium containing various concentrations of the working solutions of compounds 5a and 5b, as well as the anticancer drugs Oxaliplatin and Cisplatin, were added to the cells in the 96-well plates. 1 mM H₂O₂ solution was applied as the minimum viability (Min V) or positive control.

The untreated cells, which were not exposed to any compound or DMSO, were utilized as the negative control to determine the maximum viability (MaxV). At the time of exposure, the cell confluency was approximately 40-50%. Following exposure, the plates were incubated at 37°C for 48 hours. After the exposure time elapsed, the working solution was replaced with 200 μ L of a fresh medium consisting of MTT (3-(4,5-dimethylthiazol-2-yl)-2,5-diphenyltetrazolium bromide) (2 mg/ml), which was a mixture of 1/4 PBS and 3/4 culture medium [65]. Subsequently, the plates were incubated for an additional 4 hours at 37°C in a 5% CO₂ atmosphere. The supernatant, containing the MTT solution, was discarded, and the violet formazan crystals that had formed were dissolved by adding 200 μ L of DMSO and 25 μ L of Sorensen's glycine buffer (0.1 M glycine plus 0.1 M NaCl equilibrated at pH 10.5 using 0.1 M NaOH) into each well as the stopper [66, 67]. After shaking the plates for 40 minutes, the absorbance was measured at 570 nm using an enzyme-linked immunosorbent assay (ELISA) reader to determine the cell viability.

Statistical analysis

The experiments were conducted three times to ensure accuracy, and the results are presented as IC₅₀ \pm RSD (relative standard deviation =

[standard deviation/average] * 100). The percentage of growth inhibition for each drug concentration was determined using the formula provided. To calculate the IC₅₀ values (the concentration of the drug needed to inhibit 50% of cell growth), GraphPad PRISM software (version 9.0.0, GraphPad Software Inc.) was utilized. This software employed non-linear regression analysis to fit the data into a sigmoidal dose-response curve for each cell line.

$$\text{Growth Inhibition} = \left(1 - \frac{\text{Test } V - \text{Min } V}{\text{Max } V - \text{Min } V}\right) \times 100$$

Computational details

Two protein structures obtained from the RSCB PDB site were employed in this study. The first protein, known as 2W96 Protein, represents the crystal structure of CDK4 in complex with a D-type cyclin. The second protein, named 5LAP protein, corresponds to the p53 cancer mutant Y220C with Cys182 alkylation. To prepare the protein structures, the Schrödinger software was utilized. During the preparation process, all water molecules and ligands were eliminated from the protein structures, and optimization was performed to enhance their binding capabilities.

References

- [1] Gornowicz, A.; Szymanowska, A. *Int. J. Mol. Sci.* **2020**, 21.
- [2] Dong, J.; Li, J.; Luo, J.; Wu, W. *Eur. J. Inflamm.* **2019**, 17, 2058739219869557.
- [3] Lin, A.; Zhang, J.; Luo, P. *Front. Immunol.* **2020**, 11, 2039.
- [4] Hassanien, R.; Husein, D. Z.; Al-Hakkani, M. F. *Heliyon.* **2018**, 4, e01077.
- [5] Verdier-Pinard, P.; Lai, J.-Y.; Yoo, H.-D.; Yu, J.; Marquez, B.; Nagle, D.G.; *Mol. pharmacol.* **1998**, 53, 62.
- [6] Chinigo, G. M.; Paige, M.; Grindrod, S.; Hamel, E.; Dakshanamurthy, S.; Chruszcz, M.; *J. Med. Chem.* **2008**, 51, 4620.
- [7] Romagnoli, R.; Baraldi, P.G.; Carrion, M. D.; Cruz-Lopez, O.; Lopez Cara, C.; Basso, G.; *J. Med. Chem.* **2009**, 52, 5551.
- [8] Massarotti, A.; Theeramunkong, S.; Mesenzani, O.; Caldarelli, A.; Genazzani, A. A.; Tron, G. C. *Chem. Biol. Drug Des.* **2011**, 78, 913.
- [9] Abolhasani, H.; Zarghi, A.; Abolhasani, A.; *Lett. Drug Des. Discov.* **2014**, 11, 1149.

- [10] Dhiman, N.; Kaur, K.; Jaitak, V. *Bioorg. Med. Chem. Lett.* **2020**, 28, 115599.
- [11] Sadeghi, Z.; Abolhasani, H.; Mirjafary, Z.; Najafi, G.; Heidari, F. *J. Mol. Struct.* **2023**, 1277, 134867.
- [12] Koki, A. T.; Masferrer, J. L. *Journal of the Moffitt Cancer Center.* **2002**, 9, 28.
- [13] Li, G.; Wang, X.; Luo, Q.; Gan, C. *Mol. Med. Rep.* **2018**, 17, 6456.
- [14] Matbou Riahi, M.; Sahebkar, A.; Sadri, K.; *Int. J. Pharm.* **2018**, 540, 89.
- [15] P, DEC.; Hamy, A.S.; Lehmann-Che, J.; Scott, V.; Sigal, B.; Mathieu, M.C.; *Anticancer Res.* **2018**, 38, 1485.
- [16] Singh, S. *Int. J. Nanomedicine.* **2018**, 13, 11.
- [17] Sui, W.; Zhang, Y.; Wang, Z.; Wang, Z.; Jia, Q.; Wu, L. *Oncol. Rep.* **2014**, 31, 2252.
- [18] Xue, W.; Yang, G.; Karmakar, B.; Gao, Y. *Arab. J. Chem.* **2021**, 14, 103306.
- [19] Dacroy, S.; Fahim, A. *Carbohydr. Polym.* **2020**, 229, 115537.
- [20] Radwan, M.; Alminderej, F.; Awad, H. *Mol (Basel, Switzerland).* **2020**, 25, 255.
- [21] Wan, Y.; Fang, G.; Chen, H.; Deng, X.; Tang, Z. *Eur. J. Med. Chem.* **2021**, 226, 113837.
- [22] Shelke, RN.; Pansare, D.N.; Sarkate, A. P.; Narula, I.K.; Lokwani, D.K.; Tiwari, S.V. *Bioorg. Med. Chem. Lett.* **2020**, 30, 127246.
- [23] Zhang, B.; Hu X-T, Gu. J.; Yang, Y-S.; Duan, Y-T.; Zhu, H-L. *Bioorg. Chem.* **2020**, 105, 104390.
- [24] Mokenapelli, S.; Gutam, M.; Yerrabelli, J.R.; Irlapati, V.K.; Gorityala, N.; Sagurthi, S. R.; *Russ J Bioorg Chem.* **2020**, 46, 845.
- [25] Romagnoli, R.; Baraldi, P.G.; Salvador, M. K.; Preti, D.; Aghazadeh Tabrizi, M.; Brancale, A. *J. med. chem.* **2012**, 55, 475.
- [26] Benson, F.R. *Chem. Rev.* 1947, 41, 1.
- [27] Neochoritis, C. G.; Zhao, T.; Dömling, A. *Chem. Rev.* **2019**, 119, 1970.
- [28] Ojeda-Carralero, G. M.; Coro, J.; Valdés-Palacios, A. *Chem. Heterocycle. Cmpd.* **2020**, 56, 408.
- [29] Aureggi, V.; Sedelmeier, G. *Angew. Chem.* **2007**, 119, 8592.
- [30] Kritchenkov, A.S.; Egorov, A. R.; Krytchankou, I. S.; Dubashynskaya, N.V.; Volkova, OV.; Shakola, TV. *Int. J. Biol. Macromol.* **2019**, 132, 340.
- [31] Singh, H.; Chawla, A. S.; Kapoor, V. K.; Paul, D.; Malhotra, R. K. *Prog. Med. Chem.* **1980**, 17, 151.
- [32] Kabir, E.; Uzzaman, M. *Results. Chem.* **2022**, 100606.
- [33] Satyanarayana, B.; Sumalatha, Y.; Venkatraman, S.; Mahesh Reddy, G.; Pratap Reddy, P. *Synth. Commun.* **2005**, 35, 1979.
- [34] Van Chien, T.; Anh, N. T.; Thao, T.T. P.; Phuong, L. D.; Tham, P. T.; Tung, N. Q.; *Vietnam J. Chem.* **2019**, 57, 343.
- [35] Abelson, M. B.; Berdy, G. J.; Mundorf, T.; Amdahl, L. D.; Graves, A. L. *J. Ocul. Pharmacol. Ther.* **2002**, 18, 475.
- [36] Mishra, S.; Singh, P. *Eur. J. Med. Chem.* **2016**, 124, 500.
- [37] Popova, E.A.; Protas, A. V.; Trifonov, R.E. *Anti-Cancer Agents Med. Chem* **2017**, 17, 1856.
- [38] Wang, S-Q.; Wang, Y-F.; Xu, Z. *Eur. J. Med. Chem.* **2019**, 170, 225.
- [39] Mohite, P. B.; Pandhare, R.B.; Khanage, S.G.; Bhaskar, V. H. *J. Pharm. Res.* **2010**, 3, 43.
- [40] Lamie, P. F.; Philoppes, J.N.; Azouz, A. A.; Safwat, N.M. *J. Pharm. Res.* **2017**, 32, 805.
- [41] Holgate, S.T.; Bradding, P.; Sampson, A. P. *J. Allergy. Clin. Immunol.* **1996**, 98, 1.
- [42] Kariyone, K.; Harada, H.; Kurita, M.; Takano, T. *J. Antibiot.* **1970**, 23, 131.
- [43] Anacona, J. R.; Alvarez, P. *Transit. Met. Chem.* **2002**, 27, 856.
- [44] Gao, F.; Xiao, J.; Huang, G. *Eur. J. Med. Chem.* **2019**, 184, 111744.
- [45] Zou, Y.; Liu, L.; Liu, J.; Liu, G. *Future. Med. Chem.* **2020**, 12, 91.
- [46] Oparil, S.; Dyke, S.; Harris, F.; Kief, J.; James, D.; Hester, A.; et al. *Clin. Ther.* **1996**, 18, 797.
- [47] Julius, S.; Weber, M. A.; Kjeldsen, S. E, McInnes, G.T.; Zanchetti, A.; Brunner, H.R.; *Hypertension.* **2006**, 48, 385.
- [48] Madhavan, T.; Quinn, E.L.; Freimer, E.; Fisher, E.J.; Cox, F.; Burch, K.; *Antimicrob. Agents Chemother.* **1973**, 4, 525.
- [49] Townsend, T.R.; Reitz, B. A.; Bilker, W. B.; Bartlett, J.G. *J. Thorac. Cardiovasc. Surg.* **1993**, 106, 664.
- [50] Cloud, M. L.; Enas, G. C.; Kemp, J.; Platts-Mills, T.; Altman, L.C.; Townley, R.; *Chronic Asthma.* **1989**, 140, 1336.

- [51] Carpentier, F.; Felpin, F-X.; Zammattio, F.; Le Grogneq, E. *Org. Process Res. Dev.* **2020**, 24, 752.
- [52] Klapötke, T. M.; Witkowski, T.G. *Propellants Explos. Pyrotech.* **2015**, 40, 366-73.
- [53] Popova, E. A.; Trifonov, R. E.; Ostrovskii, V. A. *ARKIVOC: J. Org. Chem.* **2012** (i), 45.
- [54] Longbottom, D.; Franckevicius, V.; Kumarn, S.; Oelke, A.; Wascholowski, V.; Ley, S. *Chem. Inform.* **2008**, 41, 3.
- [55] Ostrovskii, V.; Popova, E.; Trifonov, R. *Adv. Heterocycl. Chem.* **2017**, 123, 1.
- [56] Voitekhovich, S.V.; Ivashkevich, O. A.; Gaponik, P. N. *Russ. J. Org. Chem.* **2013**, 49, 635.
- [57] Meanwell, N. A. *J. Med. Chem.* **2011**, 54, 2529.
- [58] Malik, M. A.; Wani, M.Y.; Al-Thabaiti, S. A.; Shiekh, R. A. *J. Incl. Phenom. Macrocycl. Chem.* **2014**, 78, 15.
- [59] Subramanian, V.; Knight, J. S.; Parelkar, S.; Anguish, L.; Coonrod, S. A.; Kaplan, M. J.; *J. Med. Chem.* **2015**, 58, 1337.
- [60] Zabrocki, J.; Smith, G.D.; Dunbar, J. B.; Iijima, H.; Marshall, G. R. *J. Am. Chem. Soc.* **1988**, 110, 5875.
- [61] Kumar, C. N. S. S. P.; Parida, DK.; Santhoshi, A.; Kota, A. K.; Sridhar, B.; Rao, V.J. *Med. Chem. Comm.* **2011**, 2, 486.
- [62] Kaushik, N.; Kumar, N.; Kumar, A.; Singh, U. K. *Immunol. Endocr. Metab. Agents Med. Chem* **2018**, 18, 3.
- [63] Meunier, B. *Acc. Chem. Res.* **2008**, 41, 69.
- [64] Herr, R. J. *Bioorg. Med. Chem.* **2002**, 10, 3379.
- [65] Abolhasani, H.; Zarghi, A.; Movahhed, T. K.; Abolhasani, A.; Daraei, B.; Dastmalchi, S. *Bioorg. Med. Chem.* **2021**, 32, 115960.
- [66] Abolhasani, A.; Biria, D.; Abolhasani, H.; Zarrabi, A.; Komeili, T. Investigation of the role of glucose decorated chitosan and PLGA nanoparticles as blocking agents to glucose transporters of tumor cells. *Int. J. Nanomed.* **2019**, 9535.
- [67] Abolhasani, A.; Heidari, F.; Noori, S.; Mousavi, S.; Abolhasani, H. *Curr. Chem. Biol.* **2020**, 14, 38.
- [68] Bauer, M.; Joerger, A.; Fersht, A. *Proc. Natl. Acad. Sci.* **2016**, 113, E5271.
- [69] Day, P.J.; Cleasby, A.; Tickle, I.J.; O'Reilly, M.; Coyle, J.E.; Holding, F.P. *Proc. Natl. Acad. Sci. U. S. A.* **2009**, 106, 4166.
- [70] Sivakumar, G. Colchicine *Curr. Med. Chem.* **2013**, 20, 892.
- [71] Lin, Z-Y.; Kuo, C-H.; Wu, D-C.; Chuang, W-L. *Kaohsiung J. Med. Sci.* **2016**, 32, 68.